BULLETIN OF THE POLISH ACADEMY OF SCIENCES
TECHNICAL SCIENCES, Vol. 68, No. 6, 2020
DOI: 10.24425/bpasts.2020.135382

Optimization of wire EDM process parameters on Al6061/Al_2O_3 composite and its surface integrity studies

T. MYTHILI[1] and R. THANIGAIVELAN[2]*

[1] Mahendra Engineering College (Autonomous), Mallasamudram-637503, Tamil Nadu, India
[2] Muthayammal Engineering College (Autonomous), Rasipuram-637408, Tamil Nadu, India

Abstract. Metal matrix composites (MMC) are finding application in many fields such as aerospace and automobile industries. This is due to their advantages such as light weight and low cost. Among all the available non-traditional machining processes, wire electric discharge machining (WEDM) is found to be a suitable method for producing complex or intricate shapes in composite materials. In this study, an aluminum metal matrix composite (AMMC) with 6% and 8% weight (wt) fraction of Al_2O_3 is prepared through the stir casting process. The fabricated AMMC specimen is machined using WEDM, considering various process parameters such as wt % of reinforcement, gap voltage (Vg), peak current (IP) wire tension (WT) and dielectric pressure (Pd). Output responses such as the machining rate (MR) and surface roughness (R_a) of the slots are analyzed by conducting L_{18} mixed orthogonal array (OA) experiments. The experiments are analyzed using techniques for order preference by similarity to ideal solution (TOPSIS) and analysis of variance (ANOVA). Based on the analyses, the optimum combination of process parameters for better MR and R_a is as follows: wt % = 6 gm, Vg = 53 V, Ip = 8 A, WT = 11 g, Pd = 13 bar. The optimum level of process parameters for MR and R_a are 1.5 mm/min and 3.648 µm, respectively. Based on ANOVA, the peak current is found to have a significant influence on MR and R_a. Moreover, based on a scanning electron microscope (SEM) image, the presence of micro-ridges, reinforcement, micro-craters, micro-cracks, recast layers and oxide formation are all analyzed on the surface being machined.

Key words: aluminum metal matrix composite (AMMC), aluminum oxide, recast layer, oxide formation, micro-crack length and micro-craters.

1. Introduction

MMC materials have been gaining importance in the most recent decade due to their advantages such as the high strength to weight ratio, good wear and corrosion resistance. These materials are finding application in various fields such as the automobile, aerospace and many other industries producing spare parts [1–4]. AMMC are fabricated through various process methods such as stir casting, powder metallurgy, pressure infiltration, spray deposition and squeeze casting. Among these, stir casting technology is a simple and inexpensive one and is suitable for mass production of composite materials [5]. For understanding the machinability of AMMC through WEDM, researchers worldwide have conducted experiments and studied the effect of process parameters. Suresh Kumar *et al*. [6] have done the WEDM experiments to optimize the process parameters such as peak current, pulse on time, wire feed rate and wt % of boron carbide on output responses like kerf width and R_a. The aluminum (6351) alloy reinforced with 5wt % SiC and with various weight content of B_4C is fabricated through the stir casting process. It is concluded that the pulse on time is the most significant factor that affects the kerf width. Patil *et al*. [7] have investigated the effect of the type of wire electrode material on the A359/SiCp composite. In this investigation, brass wire and CuZn50 coated copper wire are used and 10% to 30% of volume fraction of SiC reinforcement is used for the preparation of AMMC. Based on the results, the cutting rate is found to be greater in the case of coated wire as compared to the plain brass wire while kerf width is found to be smaller for coated wire. Sathish Kumar *et al*. [8] have investigated the effect of WEDM on Al6063 reinforced with various percentages of SiC by considering various control parameters such as pulse on time, pulse off time, gap voltage and wire feed on metal removal rate (MRR) and R_a. L_9 OA is used to carry out the experiments and it is observed that the increase in the volume % of SiC resulted in decreased MRR and increased R_a. Dey *et al*. [9] have studied the effect of machining parameters like pulse on time, pulse off time and wire speed on various wt % of fly ash reinforced with AMMC. The experimental result reveals that pulse on time and percentage of reinforcement are the most significant factors that affect all the three responses, namely cutting speed, kerf width and R_a. Lal *et al*. [10] have conducted the experiments with an Al7075/Al_2O_3/SiC hybrid composite through WEDM to determine the effect of process parameters, namely pulse on time, pulse off time, wire drum speed and pulse current. The experiments are carried out with L_{27} OA on hybrid MMC and the composite is prepared by means of the inert gas-assisted electromagnetic stir casting process. Taguchi-based grey relational analysis (GRA) is used to optimize multiple performance characteristics of hybrid MMC for R_a and kerf width. It is found that pulse on time is the major contributing factor while machining the hybrid composite. It is evident from the above literature survey that researchers have conducted machinability studies on AMMCs through WEDM, and data related to optimization of the process parameters on MR, R_a and surface topography is sparse. In the present research, AMMCs are fabricated by using an Al6061 alloy reinforced with various wt % of Al_2O_3 such as 6% and 8% through the stir

*e-mail: tvelan10@gmail.com

Manuscript submitted 2020-05-05, revised 2020-07-17, initially accepted for publication 2020-09-14, published in December 2020

casting process and cutting into suitable size for machining in WEDM. Furthermore, various WEDM parameters and levels are identified through the preliminary machining process and experiments on L_{18}-mixed OA are conducted to study the output responses. Optimization of process parameters is essential for commercialization of the WEDM process, hence multi-objective optimization techniques such as TOPSIS are used. Additionally, the most significant process parameter that affects the machining is identified using ANOVA.

2. Experimental setup

The composite materials used in the present study consist of Al6061 as the matrix material alloy, reinforced with various wt % of Al_2O_3 (6 and 8) prepared through the stir casting technique. Table 1 provides the details of chemical composition of the Al6061 alloy.

Table 1
Percentage of chemical composition of Al6061

Al	Cr	Cu	Fe	Mg	Mn	Si	Ti	Zn
96	0.35	0.40	0.70	1.20	0.15	0.80	0.15	0.25

The prepared AMMC specimens are subjected to machining through WEDM. The dimensions of the workpiece considered for the machining are 100×100×10 mm. A brass wire is used as the tool electrode material. The experiments are conducted by considering the input parameters such as gap voltage (Vg), peak current (IP) wire tension (WT) and dielectric pressure (Pd). Details of the experimental setup of WEDM are presented in Table 2.

The performance measure MR is evaluated based on the time taken for the completion of a rectangular slot for each parameter combination. Surface roughness is observed using a surface roughness meter. The levels of process parameters considered are given in Table 3. These levels are identified based on preliminary experiments.

Table 2
Details of experimental setup

Machine	WEDM make: Mitsubishi
Electrode	Brass wire (0.25mm in diameter)
Dielectric fluid	Distilled water
Machining parameters	Input current, gap voltage, dielectric pressure and wire tension
Surface roughness measuring device	Make: Mitutoyo, Model: surf test SJ-210

Table 3
Parameters and levels

No.	Parameters	Notations	Units	1	2	3
1	Wt % of reinforcement	–	–	6		8
2	Gap voltage	V_g	V	53	55	57
3	Peak current	IP	A	4	6	8
4	Wire tension	WT	G	9	10	11
5	Dielectric pressure	P_d	Bar	11	12	13

The L_{18}-mixed OA is determined based on the number of parameters and levels. In this experiment, 5 parameters are included with 1 parameter at 2 levels and the remaining 3 parameters at 3 levels; hence L_{18}-mixed OA is constructed and presented in Table 4. Figure 1 shows the photograph of the machined WEDM work piece.

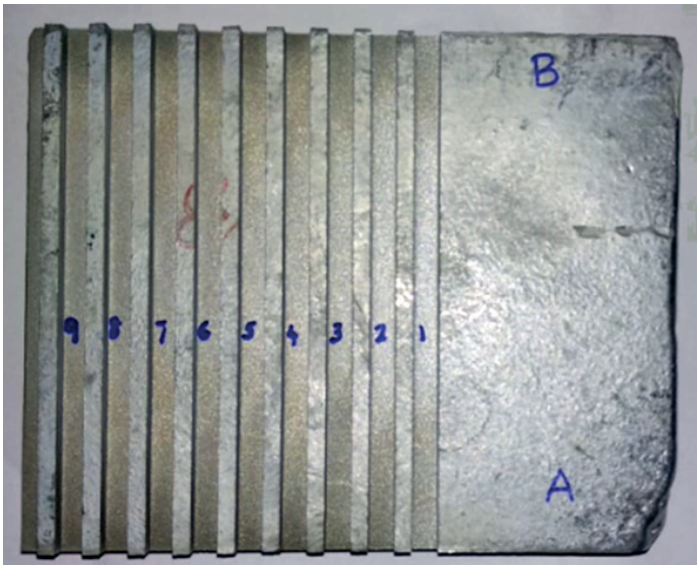

Fig. 1. Machined work piece

Table 4
L_{18}-mixed OA

Exp. No.	Wt% of reinforcement	V_g (v)	IP (A)	WT (g)	P_d (Bar)	MR mm/min	Surface roughness (R_a) µm
1	6	53	4	9	11	1.0	3.500
2	6	53	6	10	12	1.0	3.695
3	6	53	8	11	13	1.5	3.648
4	6	55	4	10	11	0.8	3.118
5	6	55	6	11	12	1.2	3.689
6	6	55	8	9	13	1.2	3.680
7	6	57	4	9	12	1.0	3.292
8	6	57	6	10	13	0.8	3.292
9	6	57	8	11	11	1.0	3.622
10	8	53	4	11	13	0.8	3.470
11	8	53	6	9	11	1.2	3.475
12	8	53	8	10	12	1.3	3.305
13	8	55	4	11	12	0.8	3.432
14	8	55	6	9	13	0.9	3.320
15	8	55	8	10	11	1.2	3.128
16	8	57	4	10	13	0.7	3.629
17	8	57	6	11	11	0.8	3.586
18	8	57	8	9	12	1.0	3.270

3. Results and discussion

The TOPSIS method proves useful for determining the best alternative from among the different alternatives available. The step-by-step procedure for the TOPSIS method is presented in [11–13].

1. Construct the decision matrix consisting of m alternatives and n criteria,

$$\text{Decision Matrix} = \begin{bmatrix} x_{11} & x_{12} & \cdots & x_{1n} \\ x_{21} & x_{22} & \cdots & x_{2n} \\ \cdots & \cdots & \cdots & \cdots \\ x_{m1} & x_{m2} & \cdots & x_{mn} \end{bmatrix}. \quad (1)$$

2. Calculate the normalized decision matrix, where the normalized value n_{ij} is calculated as follows:

$$n_{ij} = \frac{x_{ij}}{\sqrt{\sum_{j=1}^{m} x_{ij}^2}}. \quad (2)$$

j = 1, 2, 3, …, m, i = 1, 2, 3, … n.

3. Calculate the weighted normalized decision matrix, which could be determined as:

$$P_{ij} = W_i n_{ij} \quad (3)$$

j = 1, 2, 3, …, m, i = 1, 2, 3, … n.

4. Obtain positive-ideal and negative-ideal solutions from the following expressions:

$$V^+ = \left(p_1^+, p_2^+, \ldots p_n^+\right) \textit{ for } \max \textit{ values} \quad (4)$$

$$V^- = \left(p_1^-, p_2^-, \ldots p_n^-\right) \textit{ for } \min \textit{ values}. \quad (5)$$

5. Obtain separation measures by using the following expression:

$$d_j^+ = \sqrt{\sum_{i=1}^{n}\left(p_{ij} - p_i^+\right)^2} \quad (6)$$

$$d_j^- = \sqrt{\sum_{i=1}^{n}\left(p_{ij} - p_i^-\right)^2} \quad (7)$$

j = 1, 2, …, m.

6. Calculate the relative closeness coefficient by using the following equation:

$$CC_i = \frac{d_j^-}{d_j^+ + d_j^-}. \quad (8)$$

7. The CC_i values are arranged in the descending order for finding the most and the least preferred values.

The best alternative is determined from 18 alternatives and based on the attributes, the decision matrix is evaluated. The normalized decision matrix is formed by using the above TOPSIS procedures. From the normalized decision matrix, the weighted normalized decision matrix is calculated by considering the

Table 5
Normalized data, weighted normalized data, separation measures and closeness coefficient values

Expt No.	Normalized data		Weighted normalized data		Separation measures		Closeness coefficient
	MR	R_a	MR	R_a	d_j^+	d_j^-	CC_i
1	0.2282	0.2386	0.1141	0.1193	0.0585	0.0349	0.3734
2	0.2282	0.2519	0.1141	0.1259	0.0603	0.0342	0.3619
3	0.3423	0.2487	0.1712	0.1243	0.0181	0.0913	0.8348
4	0.1826	0.2125	0.0913	0.1063	0.0799	0.0227	0.2216
5	0.2739	0.2515	0.1369	0.1257	0.0394	0.0571	0.5917
6	0.2739	0.2509	0.1369	0.1254	0.0392	0.0571	0.5926
7	0.2282	0.2244	0.1141	0.1122	0.0574	0.0369	0.3914
8	0.1826	0.2244	0.0913	0.1122	0.0801	0.0179	0.1823
9	0.2282	0.2469	0.1141	0.1235	0.0596	0.0343	0.3655
10	0.1826	0.2365	0.0913	0.1183	0.0808	0.0137	0.1455
11	0.2739	0.2369	0.1369	0.1184	0.0363	0.0575	0.6130
12	0.2967	0.2253	0.1483	0.1126	0.0237	0.0697	0.7464
13	0.1826	0.2340	0.0913	0.1170	0.0806	0.0145	0.1526
14	0.2054	0.2263	0.1027	0.1132	0.0688	0.0262	0.2754
15	0.2739	0.2132	0.1369	0.1066	0.0342	0.0602	0.6376
16	0.1598	0.2474	0.0799	0.1237	0.0929	0.0022	0.0236
17	0.1826	0.2445	0.0913	0.1222	0.0815	0.0120	0.1284
18	0.2282	0.2226	0.1141	0.1113	0.0570	0.0367	0.3916

equal weightage for both the attributes. The positive-ideal and negative-ideal solutions as found from the weighted normalized decision matrix are 0.1712, 0.1063, 0.0799 and 0.1259, respectively. Separation measures of each alternative are determined using equations (6) and (7). Further, the relative closeness of a particular alternative was determined by using equation (8). The highest closeness coefficient is ranked as number 1 and from these values, it is evident that alternative 3 is the best choice for higher MR and surface quality. Based on the closeness coefficient calculated, the 12th experiment is identified to be the second best parameter combination and the 15th experiment is the third best alternative for the output responses. The optimum combination of WEDM process parameters for MR and R_a is Wt % = 6gm, V_g = 53, Ip = 8, WT = 11 and P_d = 13 bar. The MR and R_a for the optimum combination parameter levels are found to be 1.5 mm/min and 3.648 μm.

4. Result of ANOVA

The preference values obtained from the TOPSIS method are statistically analyzed by ANOVA to investigate the effects of process parameters on the output response. The most significant parameter that affects the performance characteristics is analyzed using the F-test [14]. Based on results of ANOVA in Table 6, the estimated F-values show that the peak current is the most significant factor that influences MR and surface roughness with the contribution of 47.23%. The next influencing factor that affects the machining process is gap voltage, whose contribution stands at 23.26%. The peak current plays a vital role for generation of the high energy spark required for melting and evaporation of workpiece material. Hence it is clear that proper control of electrical parameters yields the best result in the WEDM of AMMC.

Table 6
ANOVA results

Machining parameter	DOF	SS	MS	F	% of contribution
wt % of Reinforcement	1	0.03544	0.03544	1.9018	3.8406
V_g	2	0.21472	0.10736	5.7612	23.2685
IP	2	0.43584	0.21792	11.6944	47.2314
WT	2	0.02839	0.01420	0.7617	3.0766
P_d	2	0.02204	0.01102	0.2031	2.3889
Error	10	0.18630	0.01864	–	20.1941
Total	17	0.92270	0.40460	20.3222	100.0000

4.1. Effect of process parameters on MR and surface roughness. Figure 2 shows the mean effect plot for MR and R_a. It is evident that the lower level of weight percentage reinforcement shows higher MR and surface quality. Output performance increases with the decrease in the wt % of reinforcement. At

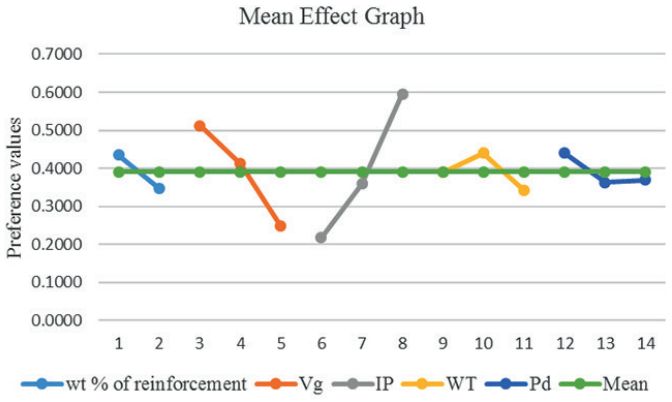

Fig. 2. Mean effect graph

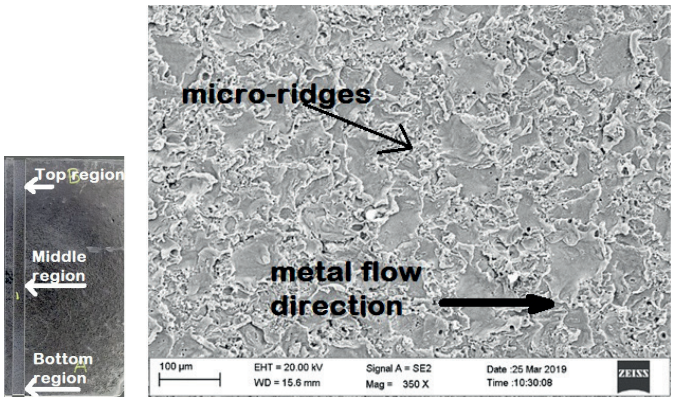

Fig. 3. Picture of machine slot & Fig. 4 SEM image of machined surface

lower wt % of reinforcement, the distribution of reinforcement in AMMC is sporadically placed all over the matrix, and hence the melting and evaporation of AMMC is faster than the one that occurs in the Al alloy. With the increase in the wt % of reinforcement, the presence of reinforcement reduces the conductivity of AMMC. This effect reduces the efficiency of spark generation and results in improper MR. Moreover, the presence of a non-conductivity zone leads to partial melting and evaporation of material, leading to recasting and de-lamination of layers. MR and surface quality are higher at lower gap voltage and increase further if gap voltage affects the output performance. The peak current shows significant influence on the response. Hence optimum selection of the electrical parameter level contributes to higher MR and surface quality. Output performance increases and decreases with wire tension. The reinforcement particle in the Al matrix during machining would exist in two states, partially melted and completely melted. The increase in wire tension contributes to the removal of completely melted material. The melting and evaporation of material depend prominently on the current and voltage, hence wire tension is considered to be a less significant factor. It is evident from Fig. 2 that the increase in dielectric pressure reduces the output performance, as it disturbs plasma generation in the machining zone.

4.2. Surface topography of the machined surface. Figure 3 shows the image of a machined slot, and the WEDMed surface is examined for its characteristics such as the micro-ridges, presence of reinforcement, micro-craters, micro-cracks, recast layers and oxide layers. The SEM images are taken at three different regions of the machined slot, namely the top region, middle region and bottom region for the optimum parameter combination.

Figure 4 depicts the surface topography of the top region of the rectangular slot for parameter combination of 6% wt of reinforcement, 53 V of gap voltage, peak current 4 A, dielectric pressure of 11 bar and wire tension of 9 g. The SEM images clearly show the generation of micro-ridges and formation of recast layers in AMMC. The pattern of forming micro-ridges is uniform towards one direction, as presented in Fig. 4. It is due to the fact that the generation of spark in a particular direction along with the plasma pressure creates the specified flow pattern of molten metal. Moreover, the cutting direction of the wire contributes to the generation of a similar type of micro-ridges, as shown in Fig. 5. The R_a value at this region is found to be at 3.5 µm and the uniform distribution of re-casted layers results in more peaks while valleys result in more R_a value.

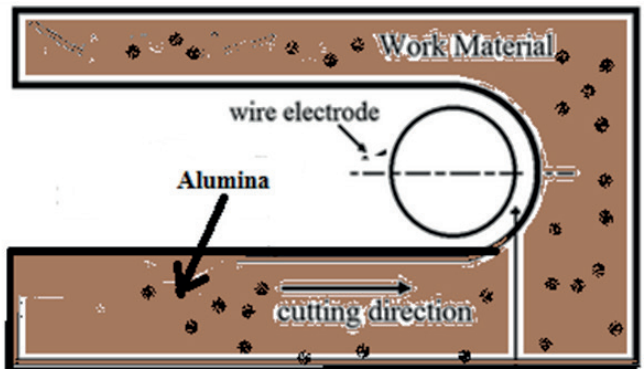

Fig. 5. Diagram of wire movement in WEDM

The SEM micrographs shown in Fig. 6 to Fig. 8 depict the middle region of the slot machined with the parameter combination for the first three experiments. It is evident from the micrograph that the presence of intense population of alumina reinforcement is noticed in the middle region of the slot as compared to top and bottom regions. Figure 9 and Fig. 10 show the SEM picture of the top and bottom regions. Furthermore, the agglomeration of alumina reinforcement in the middle region is due to the fact that during the solidification process of AMMC, the alumina particles are pushed to the central region of the specimen, contributing to agglomeration and clustering of alumina in this area. Moreover, this accumulation of reinforcement results in the breakage of fresh wire, which is predominant during machining of the middle region of the slot. The agglomeration of reinforcement and size of reinforcement significantly influence the frequency of wire breakage during the WEDM process. The optimum combination for better machining rate and surface roughness is found to be 6% weight of reinforcement, 53 V of gap voltage, peak current of 8 A, dielectric pres-

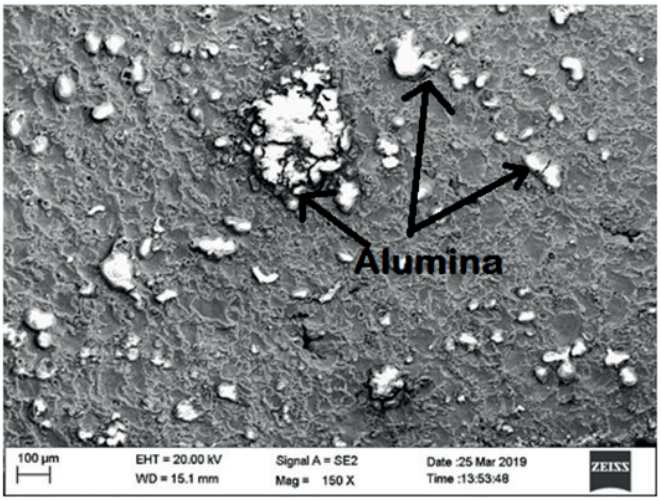

Fig. 6. SEM image of the slot for Expt No. 1

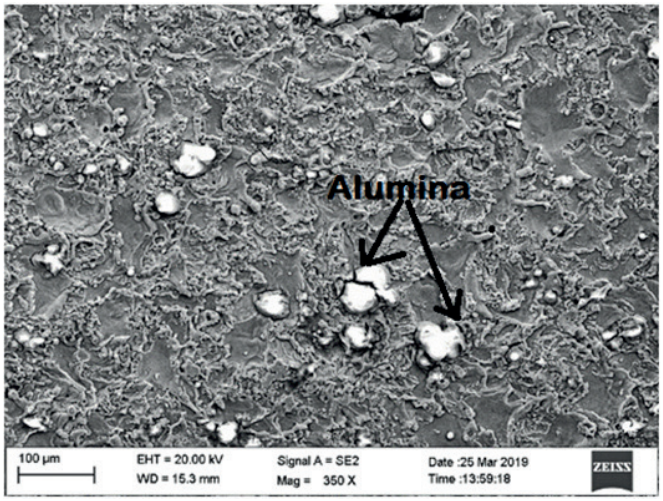

Fig. 7. SEM image of the slot for Expt No. 2

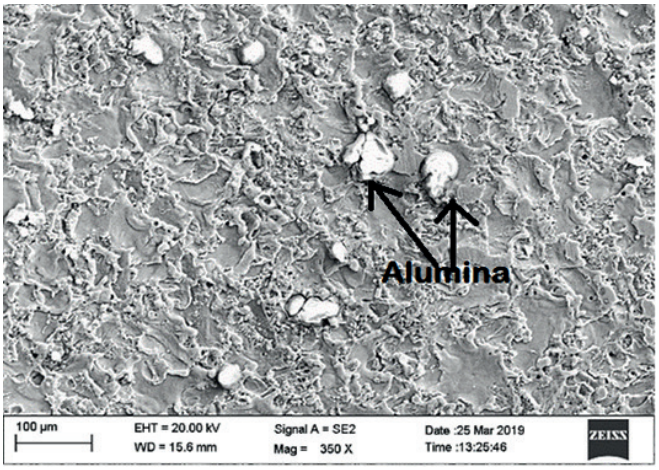

Fig. 8. SEM image of the slot for Expt No. 3

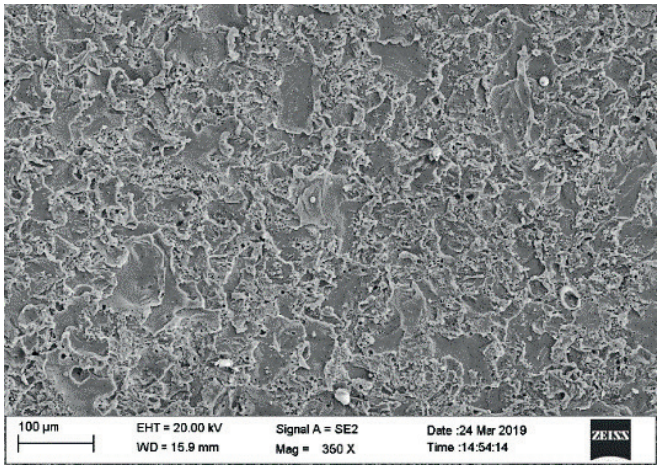

Fig. 9. Top region of the slot

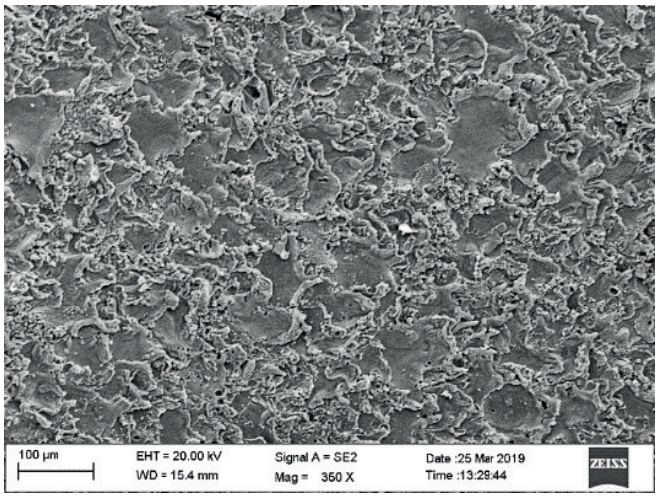

Fig. 10. Bottom region of the slot

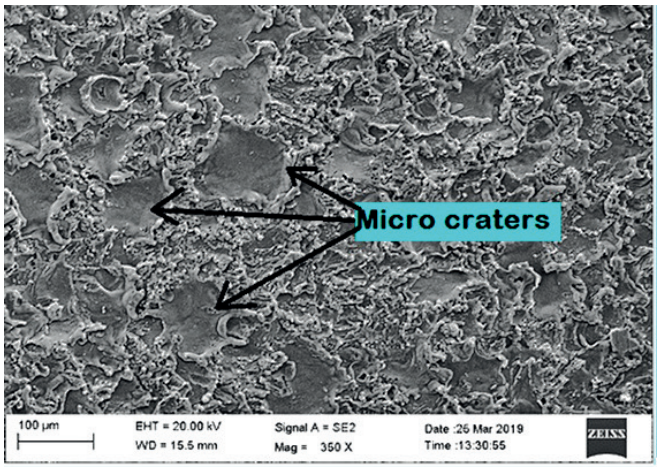

Fig. 11. SEM picture of machined surface (parameter combination of 6% wt, 53 V, 8 A, 13 bar and 11 g)

sure of 13 bar and wire tension of 11 g. The machining speed is found to be 1.5 mm/min, and also from the SEM images more micro-craters are observed, shown in Fig. 11. This can be attributed to the bulk removing of reinforcement. The reinforcement bonding in the aluminum matrix gets loosened due to heating and the bulk removal of reinforcement contributes

to more micro-craters and higher machining speed. Moreover, the sizes of the micro-craters are in the range of 80 to 120 µm**.** The optimum combination for better machining rate and surface roughness is found to be 6% weight of reinforcement, 53 V of gap voltage, peak current of 8 A, dielectric pressure of 13 bar and wire tension of 11 g. The machining speed is found to be 1.5 mm/min, and also from the SEM images more micro-craters are observed, shown in Fig. 11. This can be attributed to the bulk removing of reinforcement. The reinforcement bonding in the aluminum matrix gets loosened due to heating and the bulk removal of reinforcement contributes to more micro-craters and higher machining speed. Moreover, the sizes of the micro-craters are in the range of 80 to 120 µm**.**

In AMMC, the presence of micro-cracks is noticed mainly in the region of agglomeration of reinforcement. It is evident from Fig. 12 that the micro-cracks are initiated at the particle-matrix interfaces [15]. The SEM images clearly depict the presence of cracks near the alumina-reinforced region. The SEM micrographs presented are taken from the middle region of the slot machined for optimum combinations of process parameters. Researchers have reported that the major reason for micro-crack initiation is debonding at the reinforcement-matrix interface [16]. The length of the crack on the WEDMed surface is found to be in the range of 100–300 µm. Recast layers are nothing but the deposition of partially molten metal on the machining zone, which is not completely evaporated during sparking. The presence of recast layers on the WEDMed surface is predominately noticed in the SEM micrograph shown in Fig. 13. The generation of recast layers depends mainly on the spark energy; hence proper control of electrical parameters lowers the recast layer in the WEDM process. The gas bubbles are noticed in certain regions where reinforcement is predominantly present, as shown in Fig. 14. This is due to the fact that during the addition of alumina particles into AMMC air enters the materials along with the reinforcement. This entrapped air is released during the WEDM process and it creates the micro-void on the surfaces. Hence proper control of weight percentage and size of reinforcement have a significant effect on the generation of micro-voids.

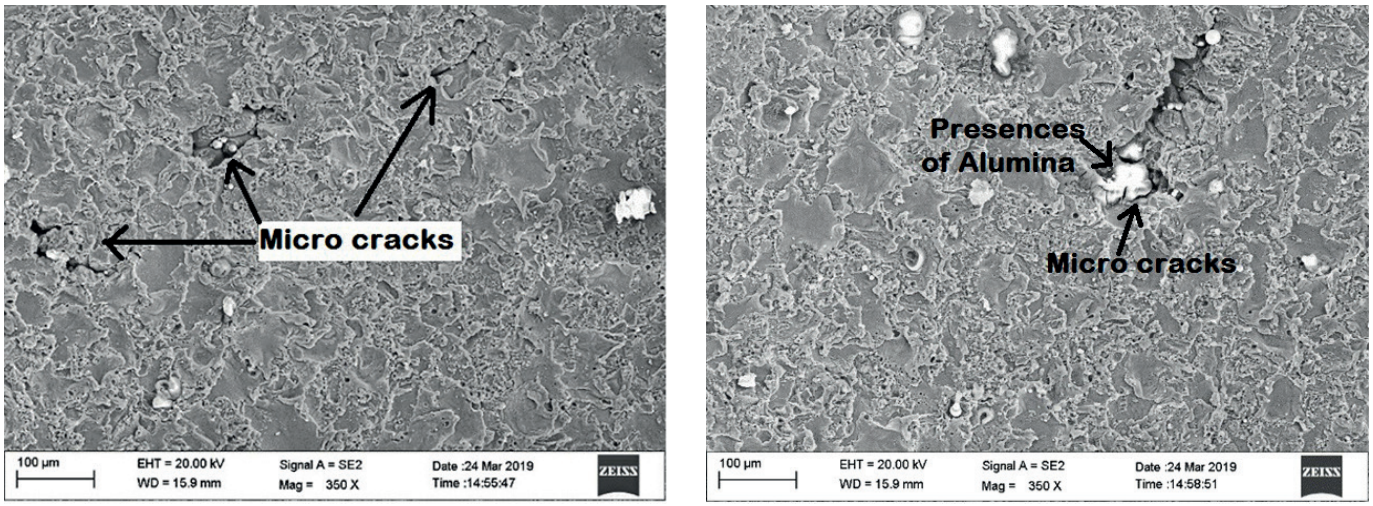

Fig. 12. Machined surface with micro cracks

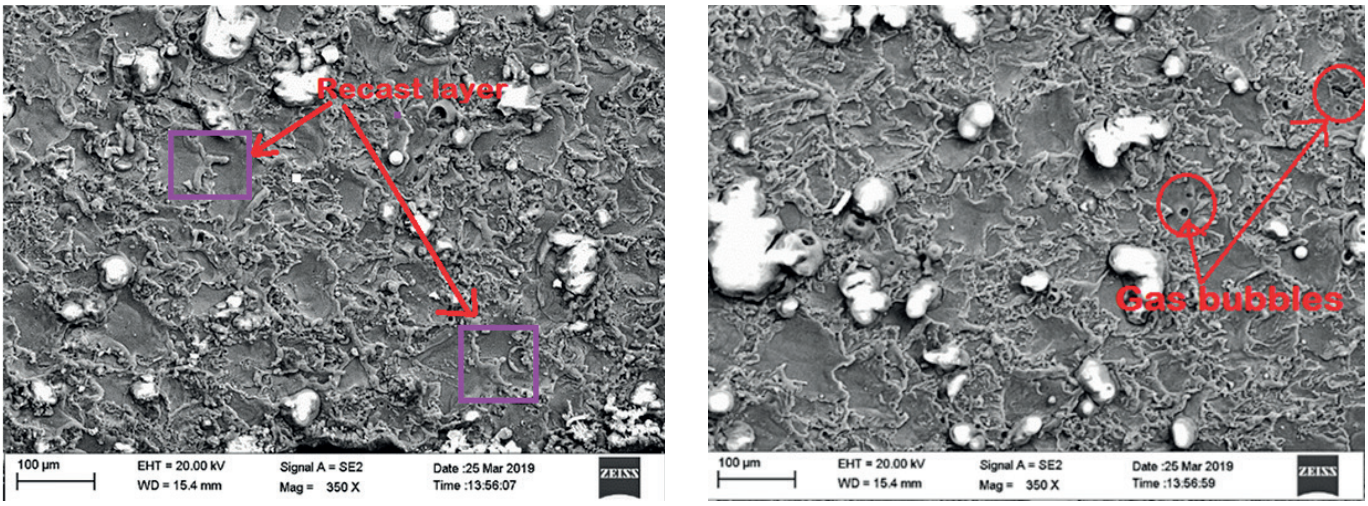

Fig. 13. Machined surface with recast layers

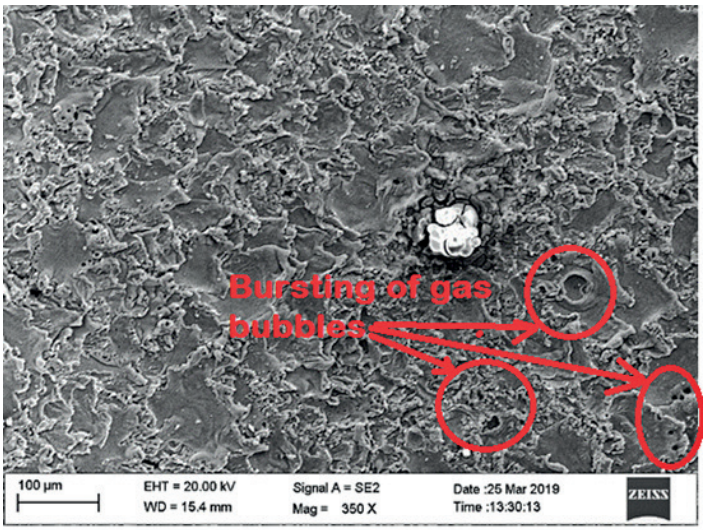

Fig. 14. Machined surface with micro-voids

Figures 15a and 15b shows the EDAX (energy dispersive X-ray) image of 6% Al_2O_3 AMMC for both the conditions, i.e. before and after machining. It is evident from Table 7 and Table 8 that there is a significant change in the percentage of oxide. The presence of oxide before machining is found to be 20.36% before machining and then it increases to 22.77% after machining. Moreover, on comparing Fig. 16a and Fig. 16b, the presence of oxide after machining for 8% is found to be 39.82%, which shows an increase of approximately 17% in oxide formation.

(a)

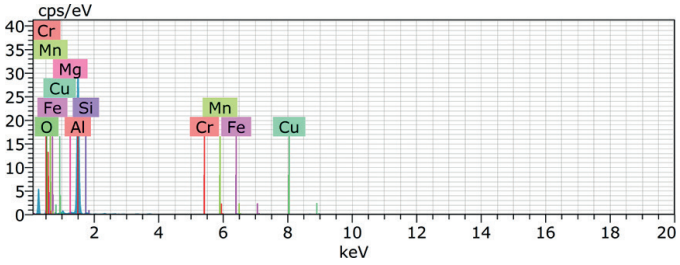

Table 7
Output of EDAX analysis – before machining (6% Al_2O_3)

EL	AN	Series	Unn. C (wt. %)	Norm. C (wt. %)	Atom. C (at %)	Error (1 Sigma) (wt. %)
Al	13	K-Series	52.43	74.03	66.05	2.54
O	8	K-Series	14.42	20.36	30.63	2.23
Fe	26	K-Series	1.31	1.85	0.80	0.08
Cu	29	K-Series	1.10	1.55	0.59	0.09
Si	14	K-Series	0.99	1.40	1.20	0.08
Mg	12	K-Series	0.49	0.69	0.69	0.06
Mn	25	K-Series	0.06	0.08	0.04	0.03
Cr	24	K-Series	0.02	0.03	0.01	0.03
		Total	70.82	100.00	100.00	

(b)

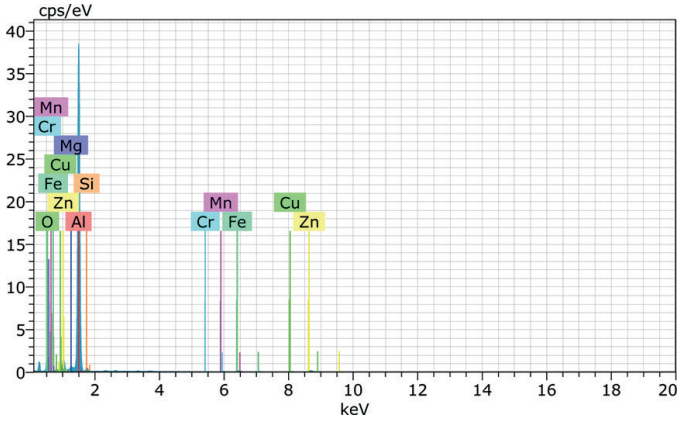

Table 8
Output of EDAX analysis – after machining (6% Al_2O_3)

EL	AN	Series	Unn. C (wt.%)	Norm. C (wt.%)	Atom. C (at%)	Error(1 Sigma) (wt.%)
AL	13	K-Series	43.60	69.18	61.89	2.11
O	8	K-Series	14.35	22.77	34.35	2.06
Zn	30	K-Series	3.20	5.08	1.88	0.15
Fe	26	K-Series	0.99	1.57	0.68	0.07
Si	14	K-Series	0.88	1.40	1.20	0.07
		Total	63.03	100.00	100.00	

Fig. 15. EDAX image (6% Al_2O_3): a) before machining, b) after machining

(a)

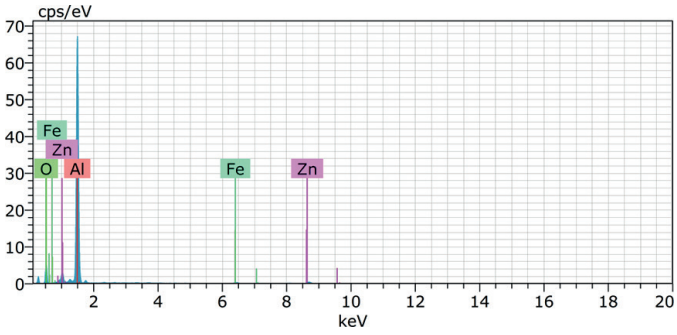

(b)

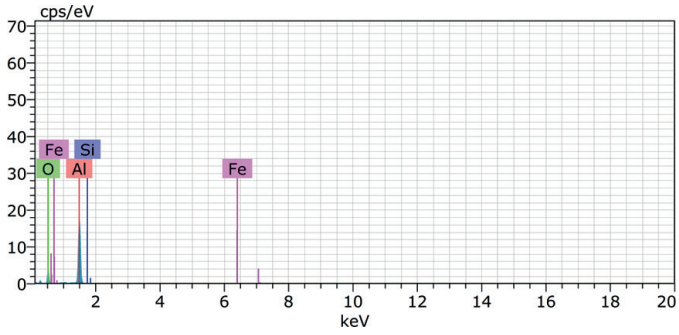

Table 9
Output of EDAX Analysis – before machining (8% Al_2O_3)

EL	AN	Series	Unn. C (wt.%)	Norm. C (wt.%)	Atom. C (at%)	Error (1 Sigma) (wt.%)
AL	13	K-Series	66.89	72.58	64.79	3.22
O	8	K-Series	20.28	22.01	33.14	2.90
Zn	30	K-Series	3.90	4.23	1.56	0.17
Fe	26	K-Series	1.09	1.18	0.51	0.07
		Total	92.16	100.00	100.00	

Table 10
Output of EDAX analysis – after machining (8% Al_2O_3)

EL	AN	Series	Unn. C (wt.%)	Norm. C (wt.%)	Atom. C (at%)	Error (1 Sigma) (wt.%)
AL	13	K-Series	53.56	58.28	45.97	2.62
O	8	K-Series	36.60	39.82	52.97	5.77
Zn	26	K-Series	0.95	1.03	0.39	0.11
Fe	14	K-Series	0.80	0.88	0.66	0.09
		Total	91.91	100.00	100.00	

Fig. 16. EDAX Image (8% Al_2O_3): a) – before machining, b) after machining

5. Conclusions

AMMCs with 6% and 8% weight fraction of Al_2O_3 are prepared through the stir casting process. They are machined using various process parameters such as wt % of reinforcement, gap voltage (Vg), peak current (IP) wire tension (WT) and dielectric pressure (Pd). Based on the TOPSIS analysis, the optimum combination for better MR and Ra is wt % = 6 gm, Vg = 53, Ip = 8, WT = 11 and Pd = 13 bar. ANOVA shows that the peak current has a significant influence on MR and Ra. The percentage of contribution of peak current is found to be 47.23. The next influencing factor that affects the machining process is gap voltage, whose contribution is 23.26%. The wire tension is considered a less significant factor.

The EDAX images for 6% and 8% of Al_2O_3 AMMC before and after machining show a significant increase in oxide formation. SEM micrographs confirm the presence of micro-ridges, reinforcement, micro-craters, micro-cracks and the recast layers on machined surface for an optimum experimental condition. The size of the micro-craters on the machined surface is in the range of 80 to 120 µm and the length of the crack is found to be in the range of 100–300 µm.

References

[1] J. Hemanth, "Quartz (SiO_2P) reinforced chilled metal matrix composite (CMMC) for automobile applications", *Mater. Des.* 30(2), 323–329 (2009).

[2] Y.C. Feng, L. Geng, P.Q. Zheng, Z.Z. Zheng, and G.S.Wang, "Fabrication and characteristic of Al-based hybrid composite reinforced with tungsten oxide particle and aluminium borate whisker by squeeze casting", *Mater. Des* 29(10), 2023–2026 (2008).

[3] C.S. Ramesh, R. Keshavamurthy, B.H. Channabasappa, and Abrar Ahmed, "Microstructure and mechanical properties of Ni–P coated Si_3N_4 reinforced Al6061 composites", *Mat. Sci. Eng. A Struct.* 502(1–2), 99–106 (2009).

[4] M. Kulczyk, J. Skiba, W. Pachla, J. Smalc-Koziorowska, S. Przybysz, and M. Przybysz. "The effect of high-pressure plastic forming on the structure and strength of AA5083 and AA5754 alloys intended for fasteners", *Bull. Pol. Ac.: Tech.* 68(4), 903–911 (2020).

[5] R. Raja, S. Jannet, and M.A. Thampy, "Synthesis and characterization of AA5083 and AA2024 reinforced with SiO_2 particles," *Bull. Pol. Ac.: Tech.* 66(2), 127–132 (2018).

[6] S. Suresh Kumar *et al.*, "Parametric optimization of wire electric discharge machining on aluminium based composite through grey relational analysis", *J. Manuf. Process.* 20(1), 33–39 (2015).

[7] G. Nilesh, P.K. Patil, D.G. Brahmankar, and D.G. Thakur, "On the effects of wire electrode and ceramic volume fraction in wire electrical discharge machining of ceramic particulate reinforced aluminium matrix composites", *Procedia of the 18th CIRP Conference on Electro Physical and Chemical Machining* 42, 286–291 (2016).

[8] D. Satishkumar *et al.*, "Investigation of wire electrical discharge machining characteristics of Al6063/SiCp composites", *Int. J. Adv. Manuf. Tech.* 56, 975–986 (2011).

[9] A. Dey, V.R. Reddy Bandi, and K.M. Pandey, "Wire electrical discharge machining characteristics of AA6061/cenosphere aluminium matrix composites using RSM", *Mater. Today Proceedings* 5(1), 1278–1285 (2018).

[10] S. Lal, S. Kumar, Z.A. Khan, A.N. Siddiquee, "Multi-response optimization of wire electrical discharge machining process parameters for Al7075/Al_2O_3/SiC hybrid composite using Taguchi-based grey relational analysis", *Proc. Inst Mech. Eng. B J. Eng. Manuf.* 229(2), 229–237 (2015).

[11] G.R. Jahanshahloo, F. Hosseinzadeh Lotfi, and M. Izadikhah, "An algorithmic method to extend TOPSIS for decision-making problems with interval data", *Appl. Math. Comput*. 175(2), 1375–1384 (2006).

[12] R. Kumar Bhuyan, B.C. Routara, and A. Kumar Parida, "An approach for optimization the process parameter by using TOPSIS Method of Al–24%SiC metal matrix composite during EDM", *Mater. Today Proceedings*, 2(4–5), 3116–3124 (2015).

[13] S. Maniraj and R. Thanigaivelan, "Optimization of electrochemical micromachining process parameters for machining of AMCs with different% compositions of GGBS using taguchi and TOPSIS methods", *T. Indian. I. Metals* 72, 3057–3066 (2019).

[14] D.C. Montgomery, *Design and Analysis of Experiments*, 4th ed., John Wiley and Sons 1997, New York.

[15] R. Thiraviam, V. Ravisankar, P. Kumar, R. Thanigaivelan, R. Arunachalam, "A novel approach for the production and characterisation of aluminium–alumina hybrid metal matrix composites", *Mater. Res. Express* 7(4), 046512 (2020).

[16] Z.Z. Chen and K. Tokaji, "Effects of Particle Size on Fatigue Crack Initiation and mall Crack Growth in SiC-Particulate Reinforced Aluminium alloy Composites", *Mater. Lett*. 58 (17–18), 2314–2321 (2004).